High-resolution Rb two-photon spectroscopy with ultrafast lasers

Tai Hyun Yoon, Adela Marian, John L. Hall, and Jun Ye

JILA, National Institute of Standards and Technology and University of Colorado
Boulder, CO 80309-0440

ABSTRACT

A two-photon transition in cold Rb atoms will be probed with a phase-coherent wide-bandwidth femtosecond laser comb. Frequency domain analysis yields a high resolution picture where phase coherence among various transition pathways through different intermediate states produces interference effects on the resonantly-enhanced transition probability. This result is supported by the time domain Ramsey interference effect. The two-photon transition spectrum is analyzed in terms of the pulse repetition rate and carrier frequency offset, leading to a cold-atom-based frequency stabilization scheme for both degrees of freedom of the femtosecond laser.

Keywords: femtosecond comb, two-photon spectroscopy, quantum interference, frequency stabilization of fs laser

1. INTRODUCTION

The recent rapid progresses in the generation of wide-bandwidth optical combs based on Kerr-lens mode-locked femtosecond (fs) lasers have opened many dramatic possibilities. The field of optical frequency metrology has been revolutionized with the capability of a single-step phase-coherent frequency bridge across several hundred THz,[1,2] leading to precision optical frequency measurements,[1,2] a direct link between optical and microwave standards,[2,3] and an absolute frequency measurement of the international optical frequency standard at 633 nm.[4] For the ultrafast science, the recent work on stabilization of the relative phase between the pulse envelope and the optical carrier[3] should lead to more exquisite control of the pulse shape and timing, opening the door for many interesting experiments in the area of extreme nonlinear optics and coherent control.

Such a remarkable measurement capability has arrived at the time when optical frequency standards based on a single ion or cold atoms are emerging as potentially the most stable clocks of any sort.[5] Although not an ultimate choice for an optical clock system, the two-photon transition of Rb atoms at 778 nm presents an attractive alternative.[6] However, our motivation to study the Rb two-photon transition with a frequency comb generated from a fs laser (fs comb) has a much broader reach than the mere improvement of the current cw-laser based two-photon system. In this paper we will show how a phase-coherent wide-bandwidth optical comb induces the desired multi-path quantum interference effect for a resonantly enhanced two-photon transition rate.[7] The analysis is carried out in both the frequency and the time domains to illustrate the novel aspect of phase-coherent pulses with a wide bandwidth that covers all the relevant intermediate states. We will discuss the consequence of these results in terms of absolute control of both degrees of freedom of the fs comb, namely the comb spacing and the carrier offset frequency. The multi-pulse interference in the time domain gives an interesting variation and generalization of the two-pulse based temporal coherent control of the excited state wavepacket.[8]

Doppler-free two-photon spectroscopy is carried out usually with two equal-frequency cw laser beams propagating in opposite directions.[9] The two-photon transition rate can be resonantly enhanced via the intermediate states with two different laser frequencies[10] or accelerated atomic beams,[11] with a small residual Doppler effect. High resolution Ramsey type two-photon spectroscopy using pulsed light has also been demonstrated,[12] with the recent extension to the cold atoms.[13] The unique feature of the present work is that the wide bandwidth optical comb allows all relevant intermediate states to resonantly participate in the two-photon excitation process, permitting the phase coherence among different comb components to induce a stronger transition rate through quantum interference.

Further author information: (Send correspondence to J.Ye)
J. Ye: E-mail: ye@jila.colorado.edu
T.H. Yoon: Permanent Address: KRISS, 1 Toryong, Yusong, Taejon 305-600, Korea; E-mail: thyoon@kriss.re.kr

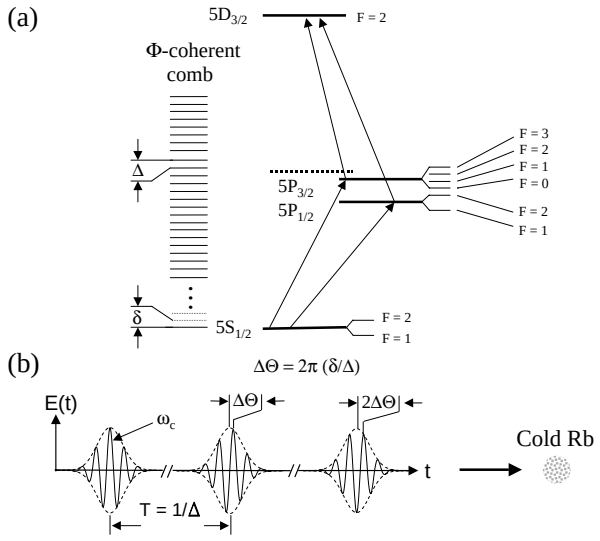

Figure 1. (a) Schematic of the relevant energy levels of the ^{87}Rb atom. (b) Sequence of mode-locked pulses. The carrier-envelope phase shift $\Delta\Theta$ is shown.

2. THEORETICAL ANALYSIS

Figure 1(a) shows the relevant ^{87}Rb energy levels involved in the two-photon transition from the ground state $5S_{1/2}$ to the excited state $5D_{3/2}$. The dipole-allowed intermediate states, $5P_{3/2}$ and $5P_{1/2}$, lie $\sim$ 2 nm and 17 nm below the virtual level (dotted line in Fig. 1(a)), respectively. Also shown is a regularly spaced comb of optical frequencies around 800 nm. The comb frequency spacing or the pulse repetition rate (Δ) is equal to the inverse of the pulse roundtrip time (T) inside the cavity. The uniformity of Δ has been demonstrated at a level of 1×10^{-17}.[1] The frequency of any comb line can thus be expressed as an integer multiple of Δ plus an offset frequency δ which arises from a difference in phase (v_p) and group (v_g) velocities of the pulses in the laser cavity. A 10 fs laser has a sufficient bandwidth to have comb components line up with corresponding hyperfine states of $5P_{3/2}$ and $5P_{1/2}$ ($\sim$ 15 nm apart) to resonantly enhance the two-photon transition. This multi-path quantum interference can be controlled by the tuning of mode spacing Δ and carrier offset frequency δ, leading to a scheme of simultaneous stabilization of both Δ and δ, and thereby the entire comb. The frequency domain analysis is complemented perfectly by the time domain multi-pulse Ramsey interference picture, as illustrated in Fig. 1(b), where the carrier-envelope phase shift $\Delta\Theta$ is also shown.

To study the dramatic enhancement of the two-photon transition rate Γ_{gf} by the resonant intermediate states and the subsequent interference among different paths, we calculate Γ_{gf} analytically in both frequency and time domains using the time-dependent second-order perturbation theory. The perturbative part of the Hamiltonian is H_I = -μE(t), where μ is the electric dipole moment and E(t) is the applied electric field. For the transition of $5S_{1/2}$ ($F'' = 2$) $\rightarrow$ $5D_{3/2}$ ($F' = 2$), we have five participating intermediate states, namely, $5P_{1/2}$ $F' = 1, 2$ and $5P_{3/2}$ $F' = 1, 2, 3$. We denote the ground state, five intermediate states, and the final excited state by $|\psi_g\rangle$, $|\psi_m\rangle$ ($m = 1-5$), and $|\psi_f\rangle$, respectively. μ_1 and μ_2 are the dipole moments associated with the transitions of $|\psi_g\rangle \rightarrow |\psi_m\rangle$ and $|\psi_m\rangle \rightarrow |\psi_f\rangle$. We note in passing that for the case of polarization-gradient cooled Rb atoms, the first-order Doppler shift can be neglected since its magnitude ($\sim$ 100 kHz) is much smaller than the natural linewidths of the intermediate states ($\sim$ 6 MHz).

2.1. Frequency Domain Analysis

For the frequency domain analysis, we express the time-dependent electric field E(t) of the fs comb as

$$E(t) = \frac{1}{2} \sum_{n=-\infty}^{\infty} E_0 \exp[-i(\omega_r + n2\pi\Delta)t] + c.c., \quad (1)$$

where $\omega_r = 2\pi(N_r\Delta + \delta)$ is a reference frequency, N_r is an integer, and we assume that the comb spectrum extends $-\infty$ to ∞ from ω_r and has the same field amplitude E_0. The atomic wave function can be expressed as

$$|\Psi(t)\rangle = \sum_l C_l(t)|\psi_l\rangle \exp(-iE_l t/\hbar) \tag{2}$$

in terms of the slowly-varying probability amplitudes $C_l(t)$ of atomic states $|\psi_l\rangle$ of energy E_l, with l covering all relevant states. In order to apply the time-dependent perturbation theory, we set $C_l(t) = C_l^{(0)}(t) + C_l^{(1)}(t) + C_l^{(2)}(t) + \cdots$, with the initial condition $C_l^{(0)}(0) = \delta_{lg}$. The interaction between the atoms and the electric field induces

$$(\frac{d}{dt} + \pi\gamma_l)C_l^{(k+1)} = -\frac{i}{\hbar}\sum_n \langle\psi_l|H_I|\psi_n\rangle \exp(i\omega_{nl}t)C_l^{(k)}, \tag{3}$$

where $\omega_{nl} = (E_l - E_n)/\hbar$ is the frequency of the transition $|\psi_n\rangle \rightarrow |\psi_l\rangle$, and γ_l are the corresponding decay terms.

We are now prepared to solve Eq. (3) for the steady-state solution of $C_f(t)$. Bjorkholm and Liao obtained an analytical solution for the second-order excited-state population $|C_f^{(2)}|^2$ for the atomic two-photon transition with a resonant or nearly-resonant intermediate state.[14] We use their basic ideas to obtain our solution for $C_f^{(2)}$, but the situation here is more general, i.e. we have a phase-coherent optical comb and multi-intermediate states. For simplicity, we restrict our attention to low optical field strength for each femtosecond comb component, so that saturation and ac Stark effects are ignored, and hence $|C_g(t)| \simeq 1, |C_m(t)| \ll 1$, and $|C_f(t)| \ll 1$. The approach we take is as follows: First we use the rotating-wave and rate-equation approximations to solve Eq. (3) for the steady-state solution $C_m^{(1)}(t)$ with the initial condition $C_l^{(0)}(0) = \delta_{lg}$. This solution for $C_m^{(1)}(t)$ is then reinserted into Eq. (3) to solve for $C_f^{(2)}(t)$. In order to keep simplicity and ease of physical interpretation we further assume that ω_{gm} and ω_{mf} are considerably different.

It is now straightforward to obtain the second-order two-photon excited-state probability amplitude $C_f^{(2)}(t)$ according to the method explained above and here is our final formula:

$$C_f^{(2)}(t) = 5\sum_p \sum_q \frac{\exp\{i[\omega_{gf} - (p+q)2\pi\Delta - 4\pi\delta]t\}}{i[\omega_{gf} - (p+q)2\pi\Delta - 4\pi\delta] + \pi\gamma_f} \sum_m \frac{\beta_1\beta_2}{i[\omega_{gm} - 2\pi(p\Delta + \delta)] + \pi\gamma_m}, \tag{4}$$

where $\beta_{1(2)} = \mu_{1(2)}E_0/2\hbar$ is the Rabi frequency associated with the transition $|\psi_g\rangle \rightarrow |\psi_m\rangle$ ($|\psi_m\rangle \rightarrow |\psi_f\rangle$), assumed to be real. In order to obtain the result of Eq. (4) we assume that almost all the atoms still remain in the ground state after the first-order interactions so that the intermediate-state populations can be neglected, because the power of each comb component is not strong enough to saturate the single-photon transitions. The two-photon transition rate is given by

$$\Gamma_{gf} = \gamma_f |C_f^{(2)}(t)|^2, \tag{5}$$

where γ_f is the natural linewidth of the excited state $|\psi_f\rangle$. In Eq. (5) Γ_{gf} has two resonance denominators. One originates from energy conservation of the two-photon transition where the sum of the two comb frequencies matches ω_{gf}; the other results from the single-photon resonance of $|\psi_g\rangle \rightarrow |\psi_m\rangle$. The linewidths of the two resonances are γ_f and γ_m, respectively. Each intermediate state provides a resonant pathway and they add coherently to yield the total transition rate Γ_{gf}, owing to the fact that different comb components are phase coherent, which is intrinsically different from the result for the single intermediate state driven by two coherent nearly-resonant fields.[14]

2.2. Time Domain Analysis

The second-order two-photon excited-state probability amplitude can be obtained independently as a solution of the Eq. (3) written in the time domain with the electric field given below. In the time domain, the train of (N+1) mode-locked pulses can be represented by

$$E(t) = \sum_{l=0}^{N} E_0 \exp[-(t - lT)^2/2\tau^2] \exp[-i\omega_c(t - lT) - il\Delta\Theta], \tag{6}$$

with $\Delta\Theta = \omega_c T(1 - v_g/v_p) = 2\pi\delta/\Delta + n2\pi$. Here ω_c is the carrier frequency, τ is the pulse width, l and n are integers. During the time periods of $lT - \tau/2$ to $lT + \tau/2$, one pulse, with its sufficiently wide bandwidth, drives

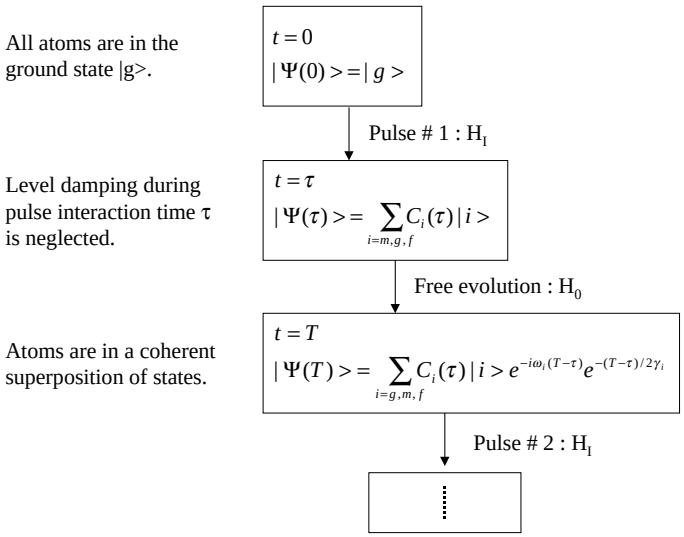

Figure 2. Time evolution sequence of the atomic state $|\Psi(0)>$ driven by the first square pulse with the pulse interaction time τ and interval between two pulses $T-\tau$, where $|i>=|g>,|m>,|f>$ refer to the ground state, intermediate states, and excited state, respectively.

the probability amplitudes of all intermediate states $C_m^{(1)}(t)$ with the first order perturbation and of the final state $C_f^{(2)}(t)$ with the second order perturbation in Eq. (3).

To reach an analytical solution, we simplify the original Gaussian pulse shape to be square, then the amplitude of the electric field in Eq. (6) becomes simply

$$\begin{aligned} E_l(t) = E_l \quad & \text{for} \quad lT \le t \le lT+\tau, \\ 0 \quad & \text{for} \quad lT+\tau \le t \le (l+1)T. \end{aligned} \tag{7}$$

Figure 2 shows the time evolution sequence of the atomic state $|\Psi(0)>$ driven by the first square pulse with the pulse interaction time τ and interval between two pulses $T-\tau$, where $|i>=|g>,|m>,|f>$ refer to the ground state, intermediate states, and excited state, respectively. We ignore the decay of the states during the pulse interaction time τ, since $\tau \ll T$ ($5 \sim 6$ orders of magnitude). In between two pulses, $lT+\tau \le t \le (l+1)T$, $l = 0$ to N, the atomic states evolve freely according to the unperturbed Hamiltonian H_0 along with the appropriate decay rates. The next pulse, with the corresponding phase shifts, will continue to build the atomic probability amplitudes in a coherent fashion. This process will of course reach a state of equilibrium since the excited state has a lifetime of $1/(2\pi\gamma_f)$. As in the frequency domain analysis, we apply the second-order perturbation theory to obtain the excited-state probability amplitude $C_f^{(2)}(NT)$. After the first pulse interaction the probability amplitudes for the intermediate states obtained from Eqs. (3) and (7) with the initial conditions $C_l^{(0)}(0) = \delta_{lg}$ are

$$C_m^{(1)}(\tau) = \beta_1 S^\tau(gm), \tag{8}$$

where

$$S^\tau(v) = \frac{\exp[i(\omega_v - s\omega_c)\tau] - 1}{\omega_v - s\omega_c} \tag{9}$$

with $s = 1$ for $v = gm, mf$, and $s = 2$ for $v = gf$. We use Eq. (8) as an initial condition for Eq. (3) to write an expression for the second-order excited-state probability amplitude $C_f^{(2)}(\tau)$ and it is easily obtained from Eq. (3) as

$$C_f^{(2)}(\tau) = \sum_m \beta_1\beta_2[S^\tau(gf) - S^\tau(mf)]\frac{1}{\omega_{gm} - \omega_c}. \tag{10}$$

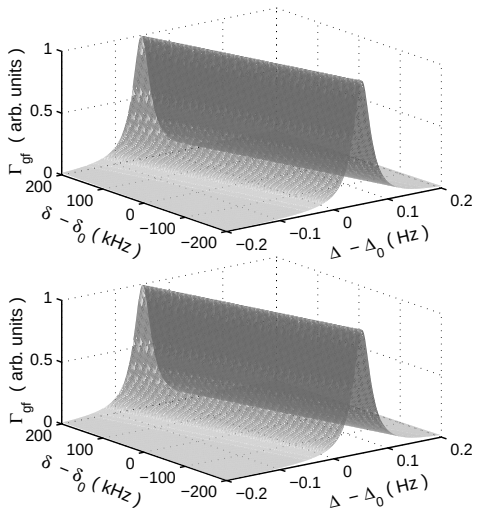

Figure 3. Γ_{gf} as a function of Δ and δ, calculated from the analytical expressions obtained in frequency domain (a) and in time domain (b). The values of Δ_0 and δ_0 are 100 MHz and 15.69 MHz, respectively, for both (a) and (b). The pulse width is 10 fs for (b)

During the time $\tau \leq t \leq T$ the atomic states evolve freely with their own decay rates and thus at time T, when the second pulse comes in, Eqs. (8) and (10) become

$$C_m^{(1)}(T) = C_m^{(1)}(\tau)\exp[-\gamma_m(T-\tau)/2], \tag{11}$$

$$C_f^{(2)}(T) = C_f^{(2)}(\tau)\exp[-\gamma_f(T-\tau)/2]. \tag{12}$$

Following the same steps for the next N pulses we are able to find the second-order probability amplitude for the excited state $C_f^{(2)}(NT)$ as

$$\begin{aligned} C_f^{(2)}(NT) &= C_f^{(2)}(\tau)\sum_{l=0}^{N}\exp[-\pi\gamma_f(N-l)T + i(\omega_{gf} - 4\pi\delta)lT] \\ &\quad + \sum_{m=1}^{5}\beta_2 S^{\tau}(mf)\sum_{l=1}^{N} C_m(lT)\exp[-\pi\gamma_f(N-l)T + i(w_{mf} - 2\pi\delta)lT], \end{aligned} \tag{13}$$

with

$$C_m(lT) = \beta_1 S^{\tau}(gm)\sum_{n=0}^{l-1}\exp[-\pi\gamma_m(l-n)T + i(\omega_{gm} - 2\pi\delta)nT]. \tag{14}$$

It is interesting to note that the phase terms in Eq. (13) depend explicitly on the carrier-envelope phase shift $\Delta\Theta$, but not on the carrier frequency ω_c, which has an effect only on the relative signal size.

2.3. Calculational Results

The measured values of the Rb transition frequencies, hyperfine intervals, and decay rates are used in the present calculations.[15] Figure 3 shows a typical Γ_{gf} as a function of Δ and δ, with curve (a) calculated from the frequency domain (Eq. 4) and (b) calculated from the time domain (Eq. 13). In the frequency domain calculation, the frequency coverage of the comb pairs to excite $|g\rangle \rightarrow |m\rangle$ and $|m\rangle \rightarrow |f\rangle$ used in the calculation far exceeds the hyperfine splittings among the intermediate states. Also the number of pulses used for the time domain calculation is larger than necessary to reach the steady state. (See Fig. 4) The agreement between the two approaches is perfect, with both graphs generated around the same nominal values of $\Delta_0 = 100$ MHz and $\delta_0 = 15.69$ MHz. The resonance

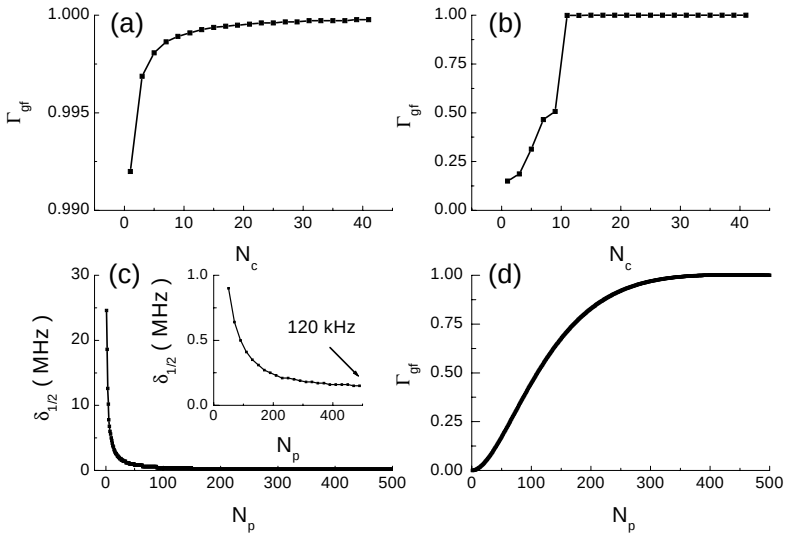

Figure 4. (a)Γ_{gf} vs. number of comb pairs N_c calculated in frequency domain. Only one intermediate state is considered. (b) Same as (a) except all five intermediate states are included. (c) Dependence of the two-photon transition linewidth $\delta_{1/2}$ on pulse number (N_p). (d) Γ_{gf} vs. pulse number (N_p).

width associated with Δ (with a fixed δ) is determined primarily from the two-photon resonance condition and is on the order of $\gamma_f/(\omega_{gf}/2\pi\Delta)$. The resonance width associated with δ is roughly on the order of γ_f (300 kHz).

To show the effect of multi-comb line contributions, i.e. multi-path quantum interference effect, we plot in Fig. 4 (a) and (b) the growth of Γ_{gf} vs. the number of participating comb pairs. The calculation is performed in the frequency domain. Figure 4 (a) shows a hypothetical case where we leave only one intermediate state to avoid quantum interference. If one of the comb pairs is resonant with the two-photon transition, we would expect all of the phase-locked comb lines to be resonant in pairs and contribute coherently to the two-photon absorption, which would result in an enhanced signal. However, as one can see from Fig. 4 (a) we find that the main contribution to the signal comes from the first comb pair with one component tuned near $|\psi_g\rangle \rightarrow |\psi_m\rangle$ and the other tuned near $|\psi_m\rangle \rightarrow |\psi_f\rangle$. And the next 15 pairs of comb lines contribute to less then 1 % of the signal level. This is understandable considering that the comb spacing Δ ($\sim$ 100 MHz) is much larger than γ_m (5 MHz). When we include all five intermediate states, the situation changes dramatically and the "saturation" curve shown in Fig. 4 (b) is less smooth, with the interference among different pathways contributing to sudden change of the signal size. Now, the first 10 pairs of comb lines need to be included for the final signal size, which depends on the frequency ratio between the comb spacing Δ and the hyperfine intervals in the $5P_{3/2}$ and $5P_{1/2}$ levels of the Rb atom and on the relative detuning of each comb pair to the intermediate levels. Figure 4 (c) and (d) illustrates the evolution of time domain interference effect as we plot the resonance linewidth and size with respect to the increasing pulse numbers. Clearly the Ramsey interference enhances the frequency resolution as more pulses participate, with the final linewidth limited basically by γ_f itself (Fig. 4 (c) and its inset), after 200 pulses or so. The signal size also reaches a stable value after a similar number of pulses (Fig. 4 (d)). The number of pulses needed to reach equilibrium is on the order of the ratio of excited state lifetime over the pulse repetition period T. The bandwidth issue of the comb can be explored with the original Gaussian pulse-shape in Eq. (6). We find that for a pulse of constant energy, the signal size remains unchanged when the pulse width τ increases, till about 30 fs, where the bandwidth becomes too small to cover the intermediate states and the signal size starts to decrease. In the calculation for Fig. 3 and Fig. 4, τ is set to be 10 fs.

3. COLD-ATOM-BASED FREQUENCY STABILIZATION SCHEME

While the results shown in Fig. 3 are informative, they are hardly useful for frequency control of the fs comb. Clearly Fig. 3 provides only one constraint for both Δ and δ and therefore we will not be able to control them independently.

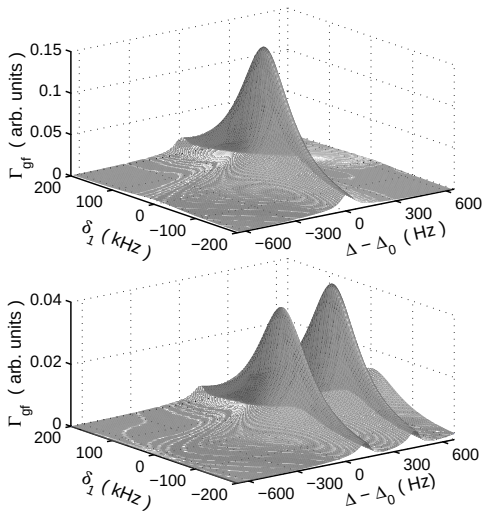

Figure 5. Γ_{gf} as functions of Δ and δ_1 (Eq. 15). All parameters are same as in Fig. 3 except $\Delta_0 = 101.851871$ MHz for (a) and $\Delta_0 = 105$ MHz for (b).

The reason lies in the fact that we have chosen the zero frequency as the reference point for both degrees of freedom associated with the comb. In other words, the effects on the comb frequency by the changes of Δ and δ are too similar and so an orthogonalized control is difficult. This situation can be remedied in practice. Optically one can adjust the laser cavity such that the frequency ω_p at which the cavity dispersion is not sensitive (to first order) to a rotating mirror lies above $\omega_{gf}/2$, i.e. virtual state (dotted line in Fig. 1) for the two-photon transition. In this case the comb components interacting with the intermediate states will be shifted down with an increasing Δ, but up with an increasing δ, leading to a possible orthogonal control. Another approach is to use electronic means to mix the control information for both Δ and δ such that two new orthogonal signals can be generated. Mathematically, this orthorgonalizaiton process amounts to a change of variables in Eq. (4), which we now rewrite as

$$C_f^{(2)}(t) = \frac{5}{2\pi} \sum_k \frac{\exp\{-4\pi i \delta_1 t\}}{i(-2\delta_1) + \gamma_f/2} \sum_m \frac{\beta_1 \beta_2}{i[\omega_{gm} - \omega_{gf}/2 - 2\pi(k\Delta + \delta_1)] + \pi\gamma_m}, \tag{15}$$

where $\delta_1 = \delta + \Delta - \mathrm{Mod}(\omega_{\mathrm{gf}}/4\pi\Delta)$. Figure 5 displays the resonance picture against δ_1 and Δ. We choose to show two representative cases with $\Delta_0 = 101.851871$ MHz for (a) and $\Delta_0 = 105$ MHz for (b). Specific values of Δ_0 are sought to have corresponding comb components tuned near a majority of the five intermediate states. Furthermore, to have a maximum enhanced peak, detunings between the five intermediate states and their respective comb lines should all have the same sign. The single peak in (a) shows an enhanced Γ_{gf} (by $3^2 = 9$ times, compared against a single state resonance) due to three constructively interfering states. (b) shows a situation where no comb lines are tuned near resonances of intermediate states and yet constructive interference still helps to enhance the signal. The resonance width associated with Δ is on the order of $\gamma_m/[(\omega_{gf}/2 - \omega_{gm})/2\pi\Delta]$. Simultaneous control of both Δ and δ is now clearly feasible. Atom-based frequency stabilization of a fs laser provides long term stability and should be an attractive complement to other approaches including lock of Δ to a microwave source,[1,2] lock of a fs laser to an optical cavity,[16] self-referenced f-2f heterodyne lock,[3] and a fs comb phase locked to an ultrastable cw laser.[17] An experimental realization of the cold-atom-based frequency stabilization of the fs laser is under way at JILA using cold ^{87}Rb atoms in a magneto-optical trap.

4. CONCLUSIONS

As a conclusion we show that the two-photon process can be dramatically enhanced through the use of a phase-coherent fs comb resonantly exciting step-wise transitions. Quantum interference among different path ways leads to the desired information of the atomic structure while providing an absolute reference for a complete control of the fs

laser. The ultrahigh resolution aspect of this approach can be understood also from the time domain analysis where a series of Ramsey-type atom-pulse interactions provide a long coherent interrogation time.

ACKNOWLEDGMENTS

We thank Dr. S. T. Cundiff for useful discussions. This work is funded by the NIST, NSF, and Research Corporation. T. H. Yoon acknowledges the financial support from JILA.

REFERENCES

1. Th. Udem, J. Reichert, R. Holzwarth, and T. W. Hänsch, "Absolute optical frequency measurement of the Cesium D_1 line with a mode-locked laser", *Phys. Rev. Lett.* **82**, pp. 3568 - 3571, 1999; Th. Udem, J. Reichert, R. Holzwarth, and T. W. Hänsch, "Accurate measurement of large optical frequency differences with a mode-locked laser", *Opt. Lett.* **24**, pp. 881 - 883, 1999.
2. S. A. Diddams, D. J. Jones, J. Ye, S. T. Cundiff, J. L. Hall, J. K. Ranka, R. S. Windeler, R. Holzwarth, Th. Udem, and T. W. Hänsch, "Direct link between microwave and optical frequencies with a 300 THz femtosecond laser comb", *Phys. Rev. Lett.* **84**, pp. 5102 - 5105, 2000.
3. D. J. Jones, S. A. Diddams, J. K. Ranka, A. Stentz, R. S. Windeler, J. L. Hall, and S. T. Cundiff, "Carrier-envelope phase control of femtosecond mode-locked lasers and direct optical frequency synthesis", *Science* **288**, pp. 635 - 639, 2000.
4. J. Ye, T. H. Toon, J. L. Hall, A. A. Madjei, J. E. Bernard, K. J. Siemsen, L. Marmet, J.-M. Chartier, and A. Chartier, "Accuracy comparison of absolute optical frequency measurement between harmonic-generation synthesis and a frequency-division femtosecond comb", *Phys. Rev. Lett.* **85**, pp. 3797 - 3800 (2000).; T. H. Yoon, J. Ye, J. L. Hall, and J.-M. Chartier, "Absolute frequency measurement of the iodine-stabilized He-Ne laser at 633 nm", *Appl. Phys. B* **72**, pp. 221 - 226 (2001).
5. J. E. Bernard, A. A. Madej, L. Marmet, B. G. Whitford, K. J. Siemsen, and S. Cundy, "Cs-based frequency measurement of a single, trapped ion transition in the visible region of the spectrum", *Phys. Rev. Lett* **82**, pp. 3228 - 3231, 1999; H. Schnatz, B. Lipphardt, J. Helmcke, F. Riehle, and G. Zinner, "First phase-coherent frequency measurement of visible radiation", *Phys. Rev. Lett.* **76**, pp. 18 - 21, 1996.
6. D. Touahri, O. Acef, A. Clairon, J.-J. Zondy, R. Felder, L. Hilico, B. de Beauvoir, F. Biraben, and F. Nez, "Frequency measurement of the $5S_{1/2}$(F=3) - $5D_{5/2}$(F=5) two-photon transition in rubidium", *Opt. Commun.* **133**, pp. 471 - 478, 1997; J. E. Bernard, A. A. Madej, K. J. Siemsen, L. Marmet, C. Latrasse, D. Touahri, M. Poulin, M. Allard, and M. Têtu, "Absolute frequency measurement of a laser at 1556 nm locked to the $5S_{1/2}$ - $5D_{5/2}$ two-photon transition in ^{87}Rb", *Opt. Commun.* **173**, pp. 357 - 364, 2000.
7. T. H. Yoon, A. Marian, J. L. Hall, and J. Ye, "Phase-coherent multilevel two-photon transition in cold Rb atoms: Ultrahigh-resolution spectroscopy via frequency-stabilized femtosecond laser", *Phys. Rev. A* **63**, 011402(R), 2001.
8. V. Blanchet, C. Nicole, M.-A. Bouchene, and B. Girard, "Temporal coherent control in two-photon transitions: from optical interferences to quantum interferences", *Phys. Rev. Lett.* **78**, pp. 2716 - 2719, 1997.
9. M. D. Levenson and N. Bloembergen, "Observation of two-photon absorption without Doppler broadening on the 3S - 5S transition in sodium vapor", *Phys. Rev. Lett.* **32**, pp. 645 - 648, 1974.
10. J. E. Bjorkholm and P. F. Liao, "Resonant enhancement of two-photon absorption in sodium vapor", *Phys. Rev. Lett.* **33**, pp. 128 - 131, 1974.
11. O. Poulsen and N. I. Winstrup, "Resonant two-photon spectroscopy in a fast accelerated atomic beam", *Phys. Rev. Lett.* **47**, pp. 1522 - 1525, 1981.
12. E. V. Baklanov and V. P. Chebotaev, "Two-photon absorption of ultrashort pulses in a gas", *Sov. J. Quantum Electron.* **7**, pp. 1252 - 1255, 1977; R. Teets, J. Eckstein, and T. W. Hänsch", *Phys. Rev. Lett.* **38**, pp. 760 - 764, 1977;
13. M. J. Snadden, A. S. Bell, E. Riis, and A. I. Ferguson, "Two-photon spectroscopy of laser-cooled Rb using a mode-locked laser", *Opt. Commun.* **125**, pp. 70 - 76, 1996.
14. J. E. Bjorkholm and P. F. Liao, "Line shape and strength of two-photon absorption in an atomic vapor with a resonant or nearly resonant intermediate state", *Phys. Rev. A* **14**, pp. 751 - 760 (1976).
15. J. Ye, S. Swartz, P. Jungner, and J. L. Hall, "Hyperfine structure and absolute frequency of the ^{87}Rb $5P_{3/2}$ state", *Opt. Lett.* **21**, pp. 1280 - 1282, 1996.

16. R. J. Jones, J.-C. Diels, J. Jasapara, ans W. Rudolph,"Stabilization of the frequency, phase, and repetition rate of an ultra-short pulse train to a Fabry-Perot reference cavity", *Opt. Commun.* **175**, pp. 409 - 418, 2000.
17. J. Ye, J. L. Hall, S. A. Diddams, "Precision phase control of an ultrawide-bandwidth femtosecond laser:a network of ultrastable frequency marks across the visible spectrum", *Opt. Lett.* **25**, pp. 1675 - 1677, 2000.